

Single-Parameter Skidding Detection and Control Specified for Electric Vehicles

Xiaodong Wu^a, Chengbin Ma^{b,a,*}, Min Xu^a, Qunfei Zhao^c, Zhiyang Cai^c

^a*School of Mechanical Engineering, Shanghai Jiao Tong University,
800 Dongchuan Road, Shanghai 200240, P. R. China*

^b*University of Michigan-Shanghai Jiao Tong University Joint Institute, Shanghai Jiao Tong University,
800 Dongchuan Road, Shanghai 200240, P. R. China*

^c*School of Electronic Information and Electrical Engineering, Shanghai Jiao Tong University,
800 Dongchuan Road, Shanghai 200240, P. R. China*

Abstract

This paper discusses a unique skidding detection and control strategy specified for electric vehicles. The anti-skid control is an exact example to explain that electric drive motors can be utilized not only for propulsion, but also as sensors and actuators in electric vehicles. This unique advantage of electric motors enables a simplified but effective anti-skid control strategy. The basic idea is to monitor and regulate a newly defined single parameter, R_{at} , the ratio of wheel equivalent linear acceleration to drive motor torque. The wheel slip level in longitudinal direction is proved to correlate to the value of R_{at} . A fuzzy-logic-based controller is then designed to regulate the variation range of R_{at} . Both simulation and experimental results validate the effectiveness of the proposed vehicle skidding detection and control. It is shown that by simultaneously using electric motors as drivers, actuators and sensors, the electric vehicles could achieve high-performance motion control with a flexible and simplified control configuration.

Keywords:

Electric vehicle, single parameter, slip level estimation, anti-skid control, fuzzy control.

1. Introduction

It is now widely recognized that vehicle electrification provides a viable solution to alleviate the emission and oil shortage problems brought by today's millions of internal combustion engine vehicles (ICEVs). Naturally most effort has been devoted to the environment and energy aspects of electric vehicles (EVs including the hybrid electric vehicles). And the widespread use of EVs is considered to largely rely on the development of long-term energy storage devices at competitive cost [1]. Meanwhile, the significance of vehicle electrification could be far beyond replacing engines and oil tanks with electric motors and batteries.

For example, the motion of EVs is produced by wheels either driven or partly driven by electric motors. Unlike conventional ICEVs, EVs are actually typical mechatronic systems. They have a configuration similar to many existing mechatronic systems such as hard disks, robots, machine tools. Motion control is one of the most important mechatronic technologies that provides quick response and high accuracy [7]. By making best use of the capability of accurate and fast motion control, future EVs would not only be clean, but also be able to achieve a higher level of safety, maneuverability and riding comfort [2, 3, 4]. Especially, four-wheel-independent-drive using in-wheel motors can enable advanced vehicle dynamics [3, 5, 6].

From the viewpoint of motion control, the unique advantages of electric motors over internal combustion engines and hydraulic braking systems could be summarized as follows:

- 1) Far less complex dynamic model
 - Approximation by a first-order system is usually sufficient for motion controller design.

*Corresponding author

Email address: chbma@sjtu.edu.cn (Chengbin Ma)

URL: <http://umji.sjtu.edu.cn/faculty/chengbin-ma/> (Chengbin Ma)

- 2) Fast torque response in milliseconds
 - Time response is 10~100 times faster than that of engines.
- 3) Easiness in obtaining accurate torque feedback
 - Generated torque is proportional with motor current, and thus easy to calculate.
- 4) Capability of generating both traction and braking forces
 - Electric motors can assist the existing hydraulic systems for a faster and more accurate braking control.
- 5) Easiness in implementing distributed in-wheel-motor systems
 - Independent torque control of each wheel enables advanced vehicle dynamics.

Compared to the engines, the electric motors have a fast and accurate response and relatively simple dynamics. Consequently, the fundamental difference between them is that the electric motors can be used not only for mobile propulsion, but also as actuators and sensors. As a simple example shown in Fig. 1, for a motor with an inertia J_m , theoretically the disturbance torque T_d (actually the vehicle traction/braking force here), can be estimated using its reverse dynamic model $J_m s$, torque and angular velocity feedback signals, T_m and ω_m . Because the electric motors may replace most of motion control actuators in conventional vehicles, high performance control of EV motion could be possible with a flexible and simplified configuration. One of those typical applications is the anti-skid control, in which the fast and accurate control and sensing capability of the electric motors could improve the performance. For conventional vehicles, the lack of accurate engine model and the hydraulic time delay of actuators make it complicated to perform quick and accurate control actions.

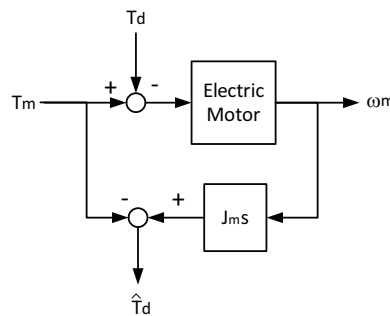


Fig. 1. An example of using electric motors as sensors

In this paper, a unique anti-skid control for electric vehicles is proposed based on monitoring and regulating a single parameter R_{at} , the ratio of wheel equivalent linear acceleration to drive motor torque. For electric motors, the feedback signals of both the angular velocity and driving torque are easy to obtain. In the anti-skid control, the electric motor is utilized not only for propulsion and actuation, but also for sensing. This unique anti-skid control is an exact example that well explains the advantages of electric motors in the motion control of EVs. The proposed parameter, R_{at} , is proved to correlate to the wheel slip ratio. Therefore vehicle velocity and acceleration measurements are not needed. Then a simplified anti-skid control strategy can be regulating R_{at} to stay within its safe range such as using fuzzy logic control. Finally, both simulation and experimental results validate the R_{at} -based single-parameter skidding detection and control.

2. Existing Anti-skid Control

2.1. Conventional ABS and TCS

For conventional ICEVs, basically two types of control strategies, two-parameter control and single-parameter control, are being used in anti-lock braking systems (ABS) and traction control systems (TCS). In the two-parameter control, the information of both vehicle velocity and wheel velocity is required. Vehicle velocity can be measured by

special devices such as accelerometer, optical sensor or GPS, etc. Those devices increase the cost and sometimes may be either not easy to implement or lose signal under certain conditions [8, 9, 10].

Most of ABS and TCS use the single-parameter control [11]. As an example, the control strategy of ABS is illustrated in Fig. 2, in which a_1 , a_2 , a_3 and a_4 are the thresholds for wheel angular acceleration determined by intensive experiments. When the wheel angular acceleration a_w reaches threshold a_2 , braking pressure is held. If a_w reaches an even lower threshold a_1 , braking pressure is decreased until a_w reaches a_2 again. The braking pressure is held between thresholds, a_2 and a_3 . Similarly, when a_w reaches threshold a_4 , braking pressure is increased, and then held between a_4 and a_3 . For TCS, besides braking the intervention may also include reducing engine torque. Through such cycles, wheel angular acceleration is controlled to keep wheel slip in a safe level without sensing vehicle velocity. Wheel slip is directly caused by excessive driving/braking torque. For ICEVs, it is difficult to estimate engine torque due to the highly complex dynamics of engines. Inadequate wheel slip estimation using only the information of wheel angular acceleration could adversely affect the control performance.

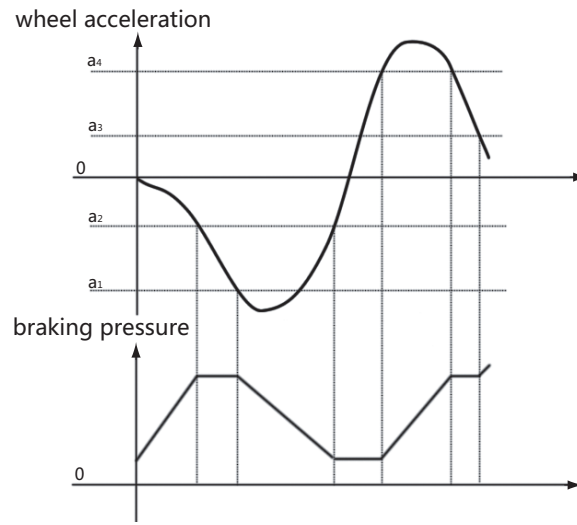


Fig. 2. The control cycles for single-parameter ABS control

2.2. Slip ratio based anti-skid control

The level of wheel slip can be described by slip ratio λ , which is defined as follows:

$$\begin{cases} \lambda = 1 - \frac{v}{v_w}, & \text{if } v < v_w \text{ and } v_w \neq 0 \text{ for acceleration} \\ \lambda = \frac{v_w}{v} - 1, & \text{if } v > v_w \text{ and } v \neq 0 \text{ for braking} \end{cases} \quad (1)$$

where v is the vehicle longitudinal velocity, and v_w is the wheel equivalent linear velocity (the product of wheel angular velocity and wheel radius).

Generally a classical PID controller can be applied to control the slip ratio at a certain desired value. Fuzzy logic control was also introduced for the anti-skid control of conventional ICEVs [12]. The objective of the fuzzy control is to regulate slip ratio λ in the positive slope region of μ - λ traction curve, or maintain the slip ratio at any target value (μ is traction coefficient) [see Fig. 4]. However, the controller inputs μ , λ and their time derivatives are difficult to measure or estimate. A fuzzy controller and a sliding mode controller were proposed to control the gradient of the μ - λ characteristic for electric vehicles [13]. Besides the difficulty in directly calculating λ , a model-based observer is needed to estimate μ .

2.3. Model based estimations

In order to avoid using the vehicle velocity information, various model-based estimations have been developed for EV's anti-skid control. A sliding-mode observer is used to estimate wheel slip and vehicle velocity under unknown

road conditions by measuring only wheel velocity [14]. The observer is based on the LuGre dynamic friction model, which helps to determine maximum transmissible torque. Based on a fixed ratio of vehicle acceleration to wheel acceleration, the maximum transmissible torque can be estimated using a disturbance observer [15] [16]. Driver's torque reference is then restrained for the prevention of vehicle skidding. A compensation scheme is also added to avoid unnecessary restraint on vehicle's acceleration performance on a normal dry road surface. Behavior model control is proposed to adapt to the nonlinear road/tire interaction [17]. The goal of the control is to force the wheel velocity to track the velocity in an ideal non-skid behavior model.

3. R_{at} -Based Skidding Detection

A unique anti-skid control specified for electric vehicles is discussed in the following sections. The sensing capability of the electric motors is utilized to estimate the wheel slip level. A single parameter, R_{at} , is then proposed for vehicle skidding detection and control, through which the measurements of vehicle velocity and acceleration are not needed any more. This newly defined single parameter enables a simplified but effective anti-skid control strategy.

3.1. Longitudinal Vehicle Dynamics

As shown in Fig. 3, the longitudinal vehicle dynamics is analyzed based on a quarter vehicle model assuming 50%-50% lateral and fore-and-aft weight distribution, as described by following equations:

$$J_w \dot{\omega}_w = T - f \cdot r, \quad (2)$$

$$M \dot{v} = F_d, \quad (3)$$

$$F_d = f, \quad (4)$$

where J_w is wheel inertia, ω_w is wheel angular velocity, T is wheel drive/braking torque, r is wheel radius, f is road/tire friction force, M is quarter-vehicle mass, v is vehicle velocity, and F_d is vehicle traction/braking force (equal to f), respectively. For the sake of simplicity, the effect of air drag on vehicle dynamics is neglected because it becomes significant only at velocities over 60 mph [18].

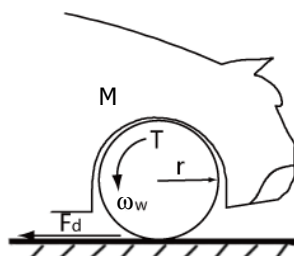


Fig. 3. The quarter-vehicle model

A common assumption is that traction coefficient μ , which is defined as a normalized traction force,

$$\mu = \frac{f}{f_n} = \frac{\text{Friction Force}}{\text{Normal Force}}, \quad (5)$$

is a nonlinear function of the relative velocity between the road and the tire. As shown in Fig. 4, the μ - λ curve has a distinct maximum value. In general the peak normalized traction force μ_p occurs at about 0.1 or 10% of the slip ratio λ . In slippery road conditions, a large driving/braking torque easily causes a rapid increase of the slip ratio, and thus the entrance into the unstable region. The sudden loss of traction (i.e. smaller μ) may lead to vehicle skidding [18].

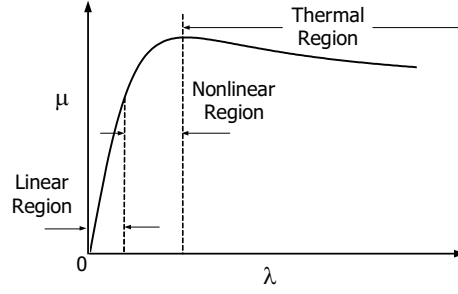


Fig. 4. Typical traction curve

3.2. Acceleration-to-torque Ratio

Compared to internal combustion engines, the torque generated by electric motors can be accurately estimated and controlled based on the feedback of the motor current. Thanks to the accurate torque feedback, a unique approach can be developed as follows for a single-parameter anti-skid control specified for EVs. The control is based on regulating the ratio of wheel acceleration to drive motor torque, i.e. R_{at} .

According to Equ. (2)-Equ. (4), the relationship between the equivalent linear wheel acceleration \dot{v}_w and the vehicle acceleration \dot{v} can be represented as:

$$\dot{v}_w = \frac{Tr - M\dot{v}r^2}{J_w}, \quad (6)$$

i.e.,

$$J_w\dot{v}_w + M\dot{v}r^2 = Tr. \quad (7)$$

Let α stands for the ratio of vehicle acceleration to wheel acceleration,

$$\alpha = \frac{\dot{v}}{\dot{v}_w}. \quad (8)$$

As previously mentioned, the electric drive motors can be used as sensors in EVs. This unique advantage could be utilized to avoid the measurements of not only vehicle velocity v , but also the acceleration \dot{v} , thus improve reliability, durability and lower the cost, etc. Here the new parameter, R_{at} , is defined as the ratio between wheel equivalent linear acceleration \dot{v}_w to wheel drive/braking torque T . According to Equ. (6) to Equ. (8), R_{at} can be represented as:

$$R_{at} \triangleq \frac{\dot{v}_w}{T} = \frac{r}{J_w + \alpha Mr^2}. \quad (9)$$

Therefore

$$\alpha = \frac{\frac{r}{R_{at}} - J_w}{Mr^2}. \quad (10)$$

For vehicle acceleration, the relationship between the slip-ratio λ and α can be described as:

$$\lambda = 1 - \frac{v}{v_w} = 1 - \frac{\int_0^t \dot{v}(t)dt}{\int_0^t \dot{v}_w(t)dt} = 1 - \frac{\int_0^t \alpha \cdot \dot{v}_w(t)dt}{\int_0^t \dot{v}_w(t)dt}. \quad (11)$$

In real applications, α can be considered as a bounded function over time t . Suppose the upper bound and lower bound of α are α_H and α_L , respectively, from Equ. (11) the range of λ can be represented as:

$$1 - \frac{\int \alpha_H \cdot \dot{v}_w(t)dt}{\int \dot{v}_w(t)dt} \leq \lambda \leq 1 - \frac{\int \alpha_L \cdot \dot{v}_w(t)dt}{\int \dot{v}_w(t)dt}. \quad (12)$$

Thus λ is within the range of $[1 - \alpha_H, 1 - \alpha_L]$. Consequently the range of the ratio R_{at} can be determined as:

$$R_{atH} = \frac{r}{J_w + \alpha_L M r^2}, \quad (13)$$

$$R_{atL} = \frac{r}{J_w + \alpha_H M r^2}, \quad (14)$$

where R_{atH} and R_{atL} are the upper and lower bounds of R_{at} , respectively. Therefore in order to avoid the measurement of vehicle velocity or acceleration, an alternative solution can be controlling R_{at} to stay within its safe range, i.e. $[R_{atL}, R_{atH}]$.

For braking, similarly

$$\lambda = \frac{v_w}{v} - 1 = \frac{\int_0^t \dot{v}_w(t) dt}{\int_0^t \dot{v}(t) dt} - 1 = \frac{\int_0^t \dot{v}_w(t) dt}{\int_0^t \alpha \cdot \dot{v}_w(t) dt} - 1, \quad (15)$$

and

$$\frac{1}{\alpha_H} - 1 \leq \lambda \leq \frac{1}{\alpha_L} - 1. \quad (16)$$

Clearly the proposed R_{at} -based anti-skid control is valid for the cases of both vehicle acceleration and braking. For the braking case, T includes the braking torque jointly generated by electric drive motor and hydraulic brake system. The estimation of hydraulic braking torque is beyond the scope of this paper. For the sake of clarity, only the anti-skid control during acceleration is discussed below. Here R_{at} is specifically defined as the ratio of wheel equivalent linear acceleration \dot{v}_w to drive motor torque T_m ,

$$R_{at} \triangleq \frac{\dot{v}_w}{T_m}. \quad (17)$$

Obviously the road/tire friction can not be infinite. Thus the available vehicle acceleration is also limited. If wheel acceleration is largely deviated from vehicle acceleration, vehicle can be considered under skidding. For example, usually a slip ratio λ ranging from 0.1 to 0.3 is considered to be safe [12]. Then according to Equ. (12), a safe range of α from 0.7 to 0.9 can be determined. If α is less than 0.7, vehicle is under skidding, while α higher than 0.9 will sacrifice vehicle acceleration performance. As shown in Equ. (10) and Fig. 5, R_{at} has a one-to-one relationship with α . Thus the wheel slip level can be directly estimated and controlled based on the new single parameter, R_{at} . Besides, for EVs, the value of R_{at} itself is easy to obtain.

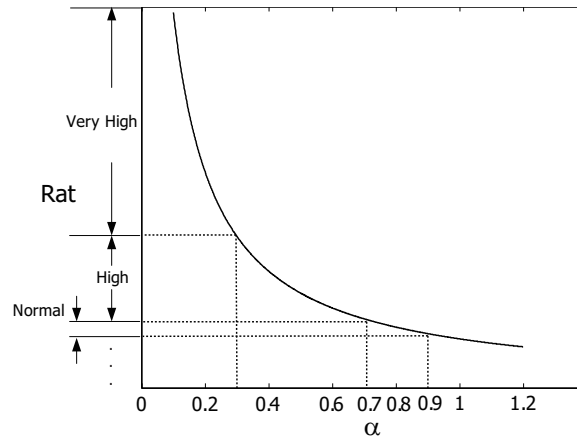


Fig. 5. The relationship between α and R_{at}

In conventional ABS and TCS systems, the wheel velocity sensor consists of a tooth gear ring and a sensor element. The resolution of the sensor is determined by the number of teeth. This number is usually less than 100 (i.e. a resolution lower than 100 pulses per revolution). For an electric vehicle, the wheel velocity can be measured using the position sensor of its drive motor, such as a resolver. The analog signal from a resolver can be converted

to digital signal with a resolution of over 1,024 pulses per revolution, namely much more precise feedback of the wheel velocity v_w . And the differentiation of the mean wheel velocity has been proved to be practical by widespread commercial applications of the conventional ABS and TCS systems [19]. The precision of the wheel acceleration computation can be further enhanced by curve fitting, interpolation, or using filters, etc. The torque generated by the drive motors is also easy to calculate based on motor current feedback. Besides the drive motor, no additional hardware such as sensors and actuators is required in the R_{at} -based anti-skid control. It is the unique advantages of electric motors that enable this simplified anti-skid control at low cost.

It is interesting to notice that in Equ. (9) the denominator $J_w + \alpha Mr^2$ directly relates to the equivalent inertia, $J_w + \alpha^2 Mr^2$, felt by drive motor when the ratio of α is constant. The slip of wheel on a low μ road surface can be considered as a sudden decrease of wheel's equivalent inertia from its nominal value. The over acceleration of wheel can be prevented by regulating the variation range of the equivalent inertia through the R_{at} -based anti-skid control.

4. R_{at} -Based Anti-Skid Controller Design

4.1. Control Strategy

For a balanced tradeoff between acceleration performance and skid prevention, regulating R_{at} within a safe range is more preferable than having a fixed value of R_{at} . Real vehicle dynamics is highly nonlinear with many uncertainties included. Fuzzy controllers have been known to have satisfactory control performance for nonlinear systems. They have been applied in many automotive electronic control systems such as engine control, traction control, and anti-lock braking systems [20, 21, 22, 23]. Therefore in this paper, a fuzzy logic anti-skid controller is introduced to regulate the range of R_{at} .

As shown by the control block diagram in Fig. 6, R_{at} is one controller input calculated by dividing feedback signals of the motor torque T_m into the wheel equivalent linear acceleration \dot{v}_w . Its rate of change is added as another input. The output of the controller is the variation of compensation torque ΔT_c , which is integrated to give the compensation torque T_c , for vehicle skid prevention. The final motor torque command T_m^* is adjusted as follows:

$$T_m^* = T_{cmd} - G \sum \Delta T_c, \quad (18)$$

where T_{cmd} is the driver's torque reference, and G is a variable coefficient over the range from zero to one. Thanks to the accurate torque control of electric motors, in motion controller design, the real generated motor torque T_m is usually considered equal to its command T_m^* [3, 15].

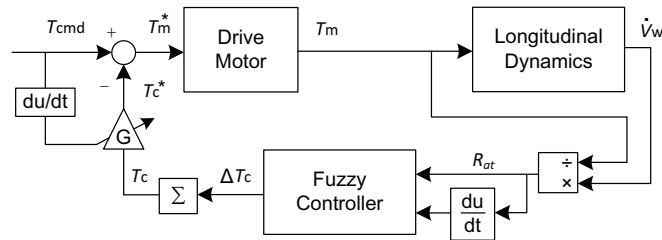


Fig. 6. The R_{at} -based fuzzy anti-skid control diagram

The relationship between α and R_{at} is illustrated in Fig. 5. If R_{at} is “very high”, it indicates a dangerous situation that may lead to a serious vehicle skid. A big increment of the compensation torque is needed to quickly decrease the motor torque T_m . On the contrary, if R_{at} is “very low”, the vehicle's acceleration performance will be adversely limited. Compared to the case of a “very high” R_{at} , this situation is not dangerous. A relatively small decrement of the output compensation torque can be applied. In order to ensure the anti-skid performance, the upper bound of R_{at} , R_{atH} , is determined under a minimum permissible α , 0.7 in this paper [refer to Equ. (13)]. Meanwhile, in real applications, even in a normal dry road surface, T_{cmd} may still be unnecessarily restrained when vehicle starts to accelerate. In order to minimize the influence on the acceleration performance, here the compensation torque T_c is adjusted by using the

increasing rate of T_{cmd} . This method is similar to the solution discussed in Ref. [15]. The compensation torque T_c in Equ. (18) is multiplied by the variable coefficient G , which is defined as:

$$G = 1 - K\dot{T}_{cmd} \text{ and } G \in [0, 1], \quad (19)$$

where \dot{T}_{cmd} is the increasing rate of T_{cmd} , and K is a compensation gain. The upper and lower bounds of G are one and zero, respectively.

The basic rules of the R_{at} -based fuzzy control can be summarized as follows:

- 1) IF R_{at} IS very high THEN ΔT_c IS greatly increased
- 2) IF R_{at} IS high THEN ΔT_c IS slightly increased
- 3) IF R_{at} IS normal THEN ΔT_c IS zero
- 4) IF R_{at} IS low THEN ΔT_c IS slightly decreased
- 5) IF R_{at} IS very low THEN ΔT_c IS greatly decreased

The relationship between R_{at} and the controller output ΔT_c is illustrated in Fig. 7. In the final fuzzy logic controller, there is another fuzzy input variable, \dot{R}_{at} , the rate of change of R_{at} [see Fig. 6]. As shown in the fuzzy rules table, Tab. 1, if R_{at} is very high and \dot{R}_{at} is negative, the compensation torque ΔT_c increases a little (i.e. SP, small positive); if R_{at} is very high and \dot{R}_{at} is zero or positive, ΔT_c increases a lot (i.e. BP, big positive). The other rules are similarly determined based on the above basic rules.

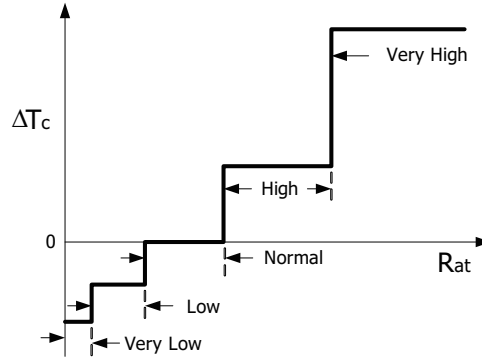


Fig. 7. The input-output relationship of the basic rules

Table 1: Fuzzy Logic Rules

R_{at}	\dot{R}_{at}		
	negative	zero	positive
very high	SP	BP	BP
high	ZERO	SP	SP
normal	SN	ZERO	SP
low	SN	SN	ZERO
very low	BN	BN	SN

The membership functions for the two input variables R_{at} and its rate of change \dot{R}_{at} , and the output variable ΔT_c are shown in Fig. 8. Basic triangle membership functions are used in this paper. The degrees of all the memberships are

based on a scale from 0 to 1, with “1” being complete membership and “0” being no membership. The membership function for R_{at} is determined based on its relationship with α [refer to Eqs. (13)(14) and Fig. 5]. For example, a “normal” R_{at} corresponds to an α between 0.7 and 0.9, i.e. a safe range of λ between 0.1 and 0.3. For the membership of the compensation torque ΔT_c , its fuzzy sets are determined through simulation and listed in Tab. 2. The fuzzy set BP is chosen as 10% of the motor torque command T_{cmd} , 2% for SP, -1% for SN (small negative), and -2% for BN (big negative). The defuzzification method used here is the center of area. Through the fuzzy control, the increment of ΔT_c is big when it is necessary to prevent vehicle skid as soon as possible, while in order to avoid adverse effect on vehicle’s acceleration performance, the decrement is relatively small because there is no danger of vehicle skid.

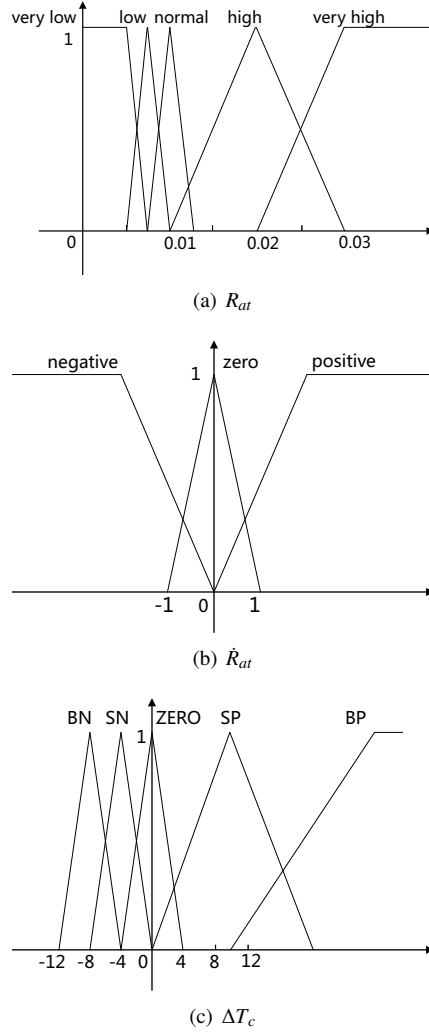


Fig. 8. Membership functions for fuzzy input and output variables

4.2. Simulation Results

Simulation is first carried out to verify the R_{at} -based anti-skid control. In the simulation, the mass of the quarter-vehicle M is 500 kg, the radius of wheel r is 0.25 m and the wheel inertia J_w (include the motor) is 1.1 kgm². The “Magic Formula” is used to describe the longitudinal road/tire interaction, namely the relationship between the slip ratio λ and the traction coefficient μ [24]. In the Pacejka’s magic model, the normalized traction force μ between the

Table 2: Fuzzy sets for the membership of the compensation torque

Fuzzy set	BP	SP	SN	BN
Percentage	10%	2%	-1%	-2%

tire and the road is modeled as:

$$\mu = c_1(\sin(c_2 \arctan(c_3 \lambda - c_4(c_3 \lambda - \arctan(c_3 \lambda))))). \quad (20)$$

Coefficient sets of c_1 , c_2 , c_3 and c_4 for various road surfaces are listed in Tab. 3. The values of the coefficients are determined by experiments [25]. In the simulation, the quarter vehicle model described in Eqs. (2)-(4) is used, in which the motor actuating system is modeled as a first-order system $1/(J_w s)$. J_w is the total inertia of the motor and the wheel. Besides, the delay of the electromechanical system between the motor torque T_m and the wheel velocity v_w is modeled as a low-pass filter (LPF), $1/(\tau s + 1)$, where τ (=0.04 second) is the time constant [15].

Table 3: The friction model coefficients for various road surfaces

Surface	c_1	c_2	c_3	c_4
Normal	1	1.9	10	0.97
Wet	0.82	2.3	12	1
Snow	0.3	2	5	1
Ice	0.1	2	4	1

For comparison purposes, the maximum transmissible torque estimation (MTTE)-based anti-skid control is also applied here. The control diagram of MTTE is shown in Fig. 9 [15]. As same as in the reference, the two time constants for the disturbance observer (DOB), τ_1 and τ_2 , in the MTTE controller are both set to 0.05 second, and the maximum transmissible torque T_{max} is determined by letting $\alpha=0.9$, i.e. a fixed acceleration ratio slightly smaller than one; the compensation for the acceleration performance is also added with a compensation gain equal to 0.1. Meanwhile, in the R_{at} -based fuzzy control, α is indirectly regulated to be within the range of 0.7 to 0.9.

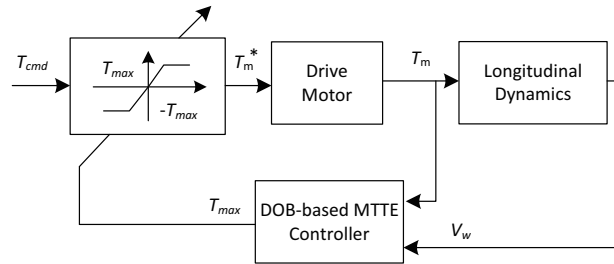


Fig. 9. The MTTE-based anti-skid control diagram

In order to verify the effectiveness of the anti-skid control, the vehicle is first simulated running on a snowy road. Motor torque command T_{cmd} is applied at 1.0 second, and increases from zero to 400 Nm within 0.5 second. Fig. 10 (a) and (b) show the simulation results of the velocities of the wheel and vehicle, and the slip ratio without anti-skid control. On the snowy road, the wheel velocity becomes much faster than the vehicle velocity. This leads to a large slip ratio of about 0.7, i.e. a serious vehicle skidding.

According to Equ. (9) and the simulation parameters, the safe range of R_{at} is determined as [0.0086, 0.0109] that corresponds to the safe range of [0.1, 0.3] for slip ratio, namely [0.7, 0.9] for α . The fuzzy sets (BP, SP, SN, and

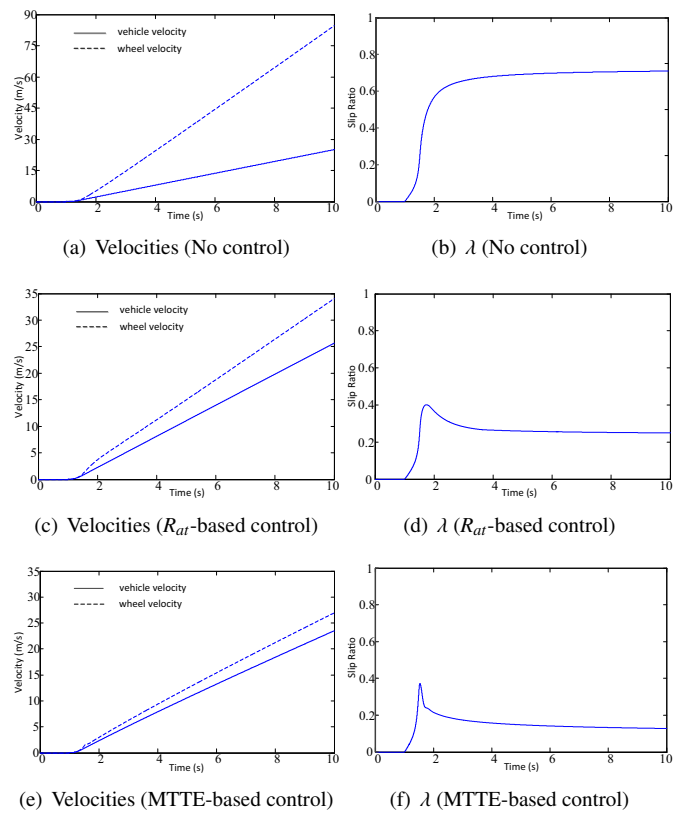


Fig. 10. Simulation results for the case of snowy road.

BN) and the membership functions of the fuzzy logic controller can also be determined accordingly as described in the previous subsection. Fig. 10 (c) and (d) show that with the fuzzy logic control, the slip ratio is well controlled to stay within the prescribed safe range of [0.1, 0.3] by properly decreasing the drive motor torque. Fig. 11 shows a stable control of the slip ratio in a long duration simulation (0-50 second). Compared with the simulation results for the MTTE-based control in Fig. 10(e) and (f), the R_{at} -based one allows the slip ratio vary in its safe range, i.e. [0.1, 0.3] here. Instead of specifying a fixed α , which might be either conservative (e.g. 0.9) or aggressive (e.g. 0.7), the R_{at} -based control provides flexibility to the variation of α within a safe range, and thus a better tradeoff between anti-skid and acceleration performances. Besides, the slip level of vehicle can be directly measured in real time by monitoring the value of R_{at} . This unique advantage has a practical importance in real applications.

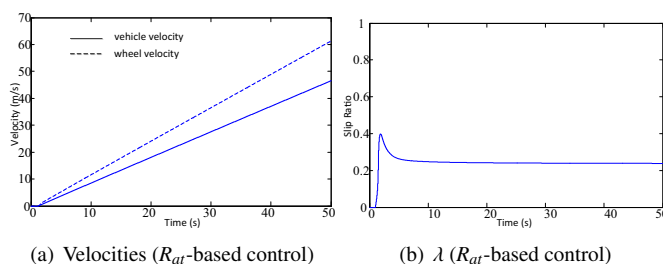


Fig. 11. Simulation results for the case of snowy road by R_{at} -based control (0-50 second).

For reference purposes, driving on an icy road is also simulated, as shown in Fig. 12. Motor torque command T_{cmd} here is increased to 150 Nm within 0.5 second from 1.0 second. Again the results show the effectiveness of the R_{at} -based fuzzy logic anti-skid control. In order to evaluate the effect of the anti-skid control in a normal case, a vehicle driving on a dry road surface is simulated. As shown in Fig. 13, by introducing the variable coefficient, G , the influence of the R_{at} -based control on the performance of normal acceleration is minimized. The compensation gain K in the simulation is set as 0.001 [refer to Equ. (19)].

All the above simulation results show that the R_{at} -based fuzzy logic anti-skid control can quickly detect and avoid potential vehicle skid. The compensation torque is properly generated to decrease the motor torque until the value of R_{at} reaches its pre-described safe range.

5. Experimental Results

As shown in Fig. 14, an experimental four-in-wheel-motor-drive electric vehicle, “SJTU EV-II”, is used to verify the proposed anti-skid control. Its specifications are listed in Tab. 4. The in-wheel motors are permanent magnet synchronized motors (PMSMs) with built-in reduction gears. The PMSM motors are under vector control and the motor drivers operate in torque control mode. A dSPACE/MicroAutoBox is used as a rapid-prototyping vehicle control unit (VCU). The control algorithm is first programmed using Matlab/Simulink, and then converted to run in MicroAutoBox under a sampling time of 0.001 second. The VCU and the motor drivers communicate through a 500K CAN (controller area network) bus. The resolution of wheel velocity feedback signal from the CAN bus is 1 rpm (revolutions per minute). As shown in Fig. 14(d), for verification purposes, a rotary optical encoder is installed in the fifth wheel. The encoder directly measures the longitudinal vehicle velocity. In the experiments, the vehicle is driven by two rear in-wheel motors.

In order to emulate a slippery road surface, two aluminum plates (10m×0.5m each) are laid on the ground, as shown in Fig. 15. The aluminum plates are sprayed with water to further lower the traction coefficient of the aluminum track. Fig. 16 shows the diagram for the R_{at} -based fuzzy logic anti-skid control in experiments, where v and v_w are the velocities of vehicle and wheel, respectively. λ is the slip ratio. T_{cmd} is the driver’s command for the output torque of each drive motor. In the experiments, T_{cmd} increases from 0 to 100Nm in 0.5 second, and then keeps constant. T_m is the final drive motor torque command adjusted by the R_{at} -based fuzzy logic anti-skid controller. Since the motors are under torque control, the real generated torque is considered equal to the torque command T_m .

The experimental results are shown in Fig. 17. The quantization error in the wheel velocity measurement can be observed due to the low resolution (1 rpm) of the feedback signal from CAN bus. In the experiments, the original

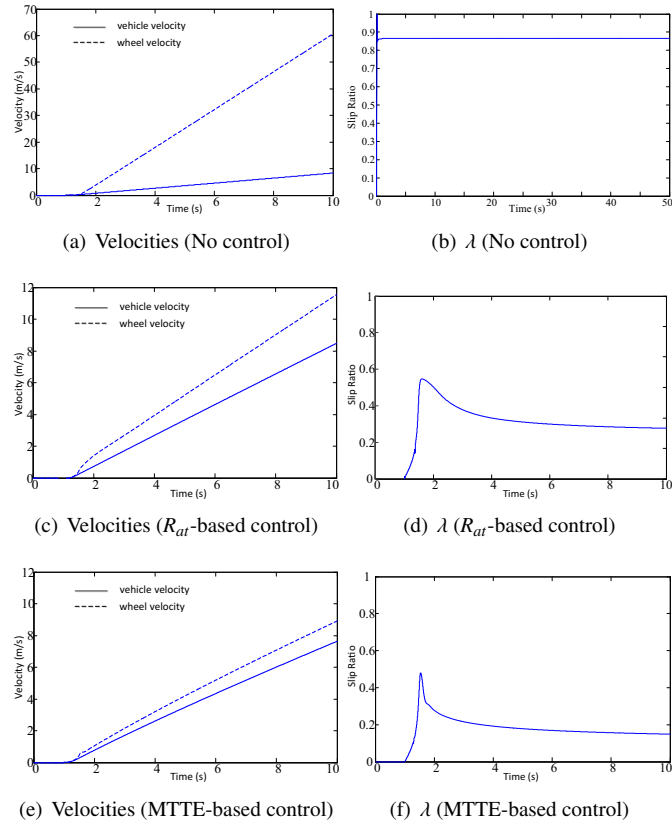


Fig. 12. Simulation results for the case of icy road (0-10 second).

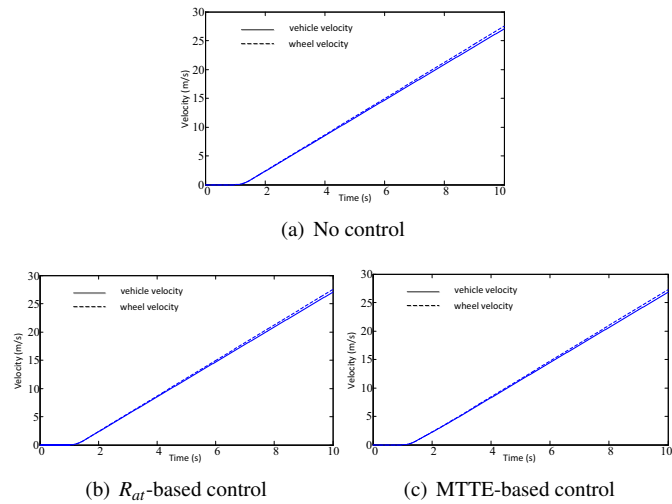


Fig. 13. Acceleration performances for the case of normal dry road.

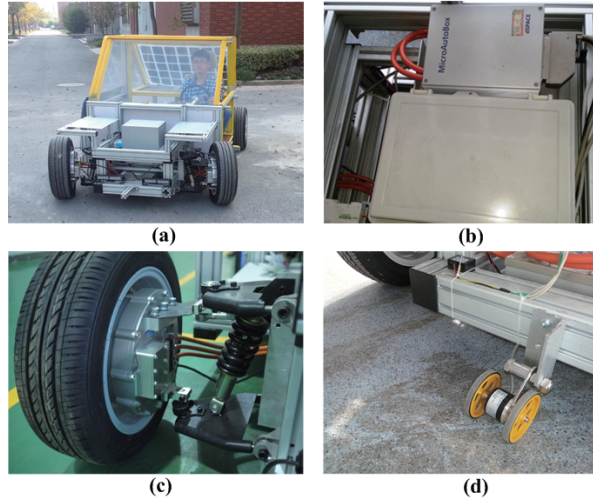


Fig. 14. The experimental electric vehicle. (a) Overview; (b) Vehicle control unit using MicroAutoBox; (c) In-wheel motor; (d) Rotary optical encoder.

Table 4: Specifications of “SJTU EV-II”

Specifications	Details
Size [m]	2.5×1.6×1.4
Weight [kg]	350
Tire	165/70 R14
Traction Motor	Four in-wheel motors (4kW each)
Motor Resolver	1,024 pulse/rev
Battery	96V Li-ion battery
Controller	dSPACE/MicroAutoBox
Optical Encoder	1,024 pulse/rev

wheel velocity signal from the CAN bus is first smoothed with a low-pass filter. The wheel acceleration is then calculated by the differentiation of the filtered wheel velocity signal. As shown in Fig. 17, because of the slippery road surface, without the anti-skid control the vehicle is in a serious skid. The vehicle eventually deviates from the track around 3.5 second due to its unstable lateral motion. After the deviation the vehicle stops skidding because it is now on a normal surface. As shown in the experimental results under the R_{at} -based fuzzy logic control, the potential danger of vehicle skid is quickly detected and prevented by properly decreasing the drive motor torque [refer to the low safe slip ratio in Fig. 17(d)]. The vehicle keeps moving straightly forward on the aluminum track. Again compared to the MTTE-based control, the R_{at} -based one achieves better acceleration performance because the acceleration ratio α is controlled within a safe range rather than at a fixed number.

6. Conclusions

This paper discusses a skidding detection and control strategy specified for electric vehicles. The unique advantages of electric motors enable a straightforward and effective anti-skid control. The basic idea is to monitor and regulate the newly defined single parameter R_{at} , the ratio of wheel equivalent linear acceleration \dot{v}_w to drive motor torque T_m . The parameter of R_{at} can be obtained in real time by using the velocity and current feedback signals of the electric drive motors. The wheel slip level in longitudinal direction is proved to correlate to the value of R_{at} . A fuzzy logic controller is designed to regulate the variation range of R_{at} , and thus achieve a balanced tradeoff between anti-skid control and vehicle acceleration performances.



Fig. 15. Experimental site with two aluminum plates.

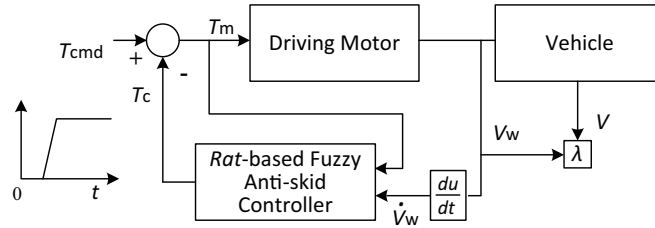


Fig. 16. Diagram for the R_{ar} -based fuzzy logic anti-skid control in experiments.

Both the simulation and experiments validate the effectiveness of the proposed single-parameter vehicle skidding detection and control. The results well explain that by simultaneously using electric motors as drivers, actuators and sensors, electric vehicles can achieve high-performance motion control with a flexible and simplified control configuration. Future works may include applying the R_{ar} -base control in braking case. The delicate interaction between hydraulic braking system and electric drive motor needs to be studied.

Acknowledgment

The authors would like to thank National Science Foundation of China [grant number 51305259 and 51375299], for supporting this work.

References

- [1] F. V. Conte. "Battery and battery management for hybrid electric vehicles: a review," *Elektrotechnik & Informationstechnik*, vol. 123, no. 10, pp. 424-431, Sep. 2006.
- [2] T. Saitoh, C. Tai, Y. Hori. "Realtime Generation of SMART Speed Pattern for EVs Taking Driver's Command Change into Account". Proceedings of the 8th IEEE International Workshop on Advanced Motion Control, pp. 81-85, March 25-28, 2004, Kawasaki, Japan.
- [3] Y. Hori. "Future Vehicle Driven by Electricity and Control - Research on Four-Wheel-Motored 'UOT Electric March II'". *IEEE Transactions on Industrial Electronics*, Vol. 51, No. 5, October 2004, pp. 954-962.
- [4] C. Ma, M. Xu, H. Wang. "Dynamic Emulation of Road/Tyre Longitudinal Interaction for Developing Electric Vehicle Control Systems". *Vehicle System Dynamics*, Vol. 49, No. 3, 2011, pp. 433-447.
- [5] Z. Shuai, H. Zhang, J. Wang, J. Li, M. Ouyang. "Lateral motion control for four-wheel-independent-drive electric vehicles using optimal torque allocation and dynamic message priority scheduling". *Control Engineering Practice*, Vol. 24, 2014, pp. 55-66.
- [6] H. Zhang, X. Zhang, J. Wang. "Robust gain-scheduling energy-to-peak control of vehicle lateral dynamics stabilisation". *Vehicle System Dynamics*, 2014 (ahead-of-print), pp. 1-32.
- [7] K. Ohnishi, M. Shibata, T. Murakami. "Motion Control for Advanced Mechatronics". *IEEE/ASME Transactions on Mechatronics*, Vol. 1, March 1996, pp. 56-67.
- [8] J. D. Turner and L. Austin. "Sensors for Automotive Telematics", *Measurement Science & Technology*, Vol. 11, No. 2, pp. 58-79, 2000.
- [9] G. A. MacDonald. "A Review of Low Cost Accelerometers for Vehicle Dynamics", *Sensors and Actuators A: Physical*, Vol. 21, No. 1-3, pp. 303-307, February 1990.
- [10] D. M. Bevly, J. C. Gerdes, C. Wilson, G. Zhang. "The use of GPS based velocity measurements for improved vehicle state estimation", Proceedings of American Control Conference, Vol. 4, pp. 2538-2542, Jun. 28, 2000-Jun. 30, 2000, Chicago, IL, USA.
- [11] U. Kiencke, L. Nielsen. "Automotive Control Systems", ISBN 3-540-23139-0 Springer, Berlin, Heidelberg, New York, 2006.

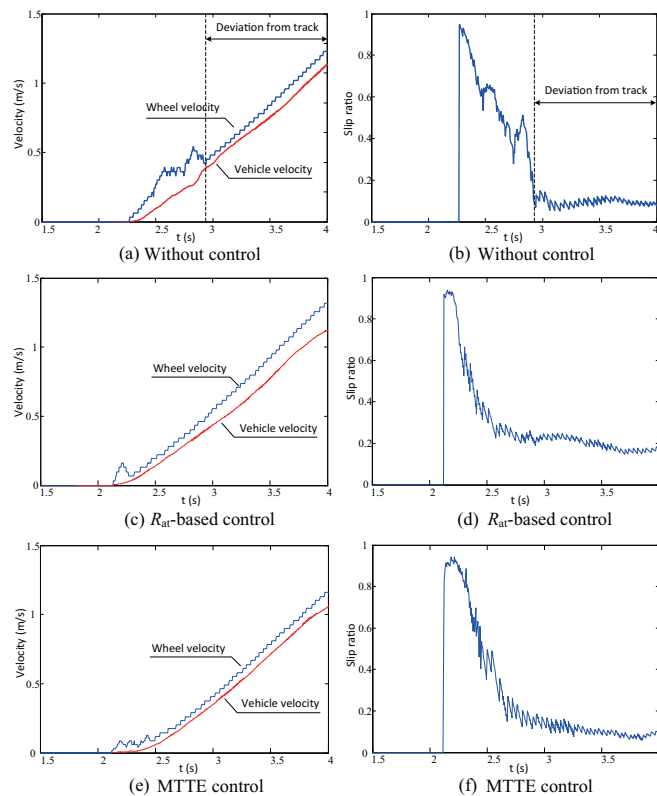


Fig. 17. Experimental results.

- [12] M. Bauer, M. Tomizuka. "Fuzzy Logic Traction Controllers And Their Effect On Longitudinal Vehicle Platoon Systems". *Vehicle System Dynamics*, Vol. 25, No. 4, April 1996, pp. 277-303.
- [13] V. D. Colli, G. Tomassi, M. Scarano. "Single Wheel Longitudinal Traction Control for Electric Vehicles". *IEEE Transaction on Power Electronics*, Vol. 21, No. 3, May 2006, pp. 799-808.
- [14] G. A. Magallan, C.H. De Angelo, and G.O. Garcia. "Maximization of the Traction Forces in a 2WD Electric Vehicle". *IEEE Transactions on Vehicular Technology*, Vol. 60, No. 2, 2011, pp. 369-380.
- [15] D. Yin, S. Oh, Y. Hori. "A Novel Traction Control for EV Based on Maximum Transmissible Torque Estimation". *IEEE Transactions on Industrial Electronics*, Vol. 56, No. 6, June 2009, pp. 2086-2094.
- [16] J. S. Hu, D. Yin and F. R. Hu. "Electric vehicle traction control: A new MTTE methodology". *IEEE Industry Applications Magazine*, Vol. 18, No. 2, 2012, pp. 23-31.
- [17] K. Hartani, M. Bourahla, Y. Miloud. "New Anti-skid Control for Electric Vehicle Using Behavior Model Control based on Energetic Macroscopic Representation", *Journal of Electrical Engineering*, Vol. 59, No. 5, 2008, pp. 225-233.
- [18] T. D. Gillespie, L. Q. Zhao, D. F. Jin. "Fundamentals Of Vehicle Dynamics (Chinese Vision)", Tsinghua University Press, 2006.
- [19] L. Austin, D. Morrey. "Recent Advances in Antilock Braking Systems and Traction Control Systems". *Proceedings of the Institute of Mechanical Engineers*, VOL. 214, Part D, 2000, pp. 625-638.
- [20] G. J. Vachtsevanos, S. S. Farinwata and D. K. Pirovolou. "Fuzzy logic control of an automotive engine". *IEEE Control Systems*. Vol. 13, No. 3, 1993, pp. 62-82.
- [21] P. Khatun, C. M. Bingham, N. Schofield, and P. H. Mellor. "Application of Fuzzy Control Algorithms for Electric Vehicle Antilock Braking/Traction Control Systems". *IEEE Transactions on Vehicular Technology*, Vol. 52, No. 5, 2003, pp. 1356-1364.
- [22] G. F. Mauer. "A fuzzy logic controller for an ABS braking system". *IEEE Transactions on Fuzzy Systems*, Vol. 3, No. 4, 1995, pp. 381-388.
- [23] W. Wei-Yen, L. I-Hsum, C. Ming-Chang, S. Shun-Feng and H. Shi-Boun. "Dynamic Slip-Ratio Estimation and Control of Antilock Braking Systems Using an Observer-Based Direct Adaptive Fuzzy-Neural Controller". *IEEE Transactions on Industrial Electronics*, Vol. 56, No. 5, 2009, pp. 1746-1756.
- [24] Canudas de Wit C., Tsiotras P., Velenis E., Basset M. and Gissinger G. "Dynamic Friction Models for Road/Tire Longitudinal Interaction". *Vehicle System Dynamics*, Vol. 39, No. 3, 2003, pp. 189-226.
- [25] Short M., Port M. J. and Huang Q. "Simulation of Vehicle Longitudinal Dynamics". *Technical Report ESL 04/01*, Embedded Systems Laboratory, University of Leicester, United Kingdom, 2004.